J Oceanogr (2011) 67:315–321
DOI 10.1007/s10872-011-0039-y

ORIGINAL ARTICLE

The Indian Ocean's asymmetric effect on the coupling of the Northwest Pacific SST and anticyclone anomalies during its spring–summer transition after El Niño

Haibo Hu · Jie He · Qigang Wu · Yuan Zhang

Received: 8 December 2010 / Revised: 6 January 2011 / Accepted: 30 April 2011 / Published online: 4 June 2011
© The Oceanographic Society of Japan and Springer 2011

Abstract By comparing different climatologies in El Niño decaying summer with regard to the presence of Indian Ocean Basin (IOB) warming, we studied the effect of IOB warming on the Northwest Pacific sea surface temperature (SST) anomalies and the coupling process with the surface wind. Zonal asymmetric coupling feedback in the west and east of the Northwest Pacific were caused by the asymmetric spring–summer transition of the background tropical atmospheric circulation. Although the westward wind anomaly caused by the remote effect of IOB warming is found in the whole Northwest Pacific, reversal of the mean background surface winds in the western part leads to negative wind-evaporation SST (WES), whereas sustained trade winds lead to positive WES in the eastern part. The east–west SST gradient resulting from this zonal asymmetric evolution of SST sets off more positive feedback that strengthens the local anticyclone easterly anomalies.

Keywords IOB · Northwest Pacific · Asymmetric effect · Spring–summer transition

1 Introduction

Long ago scientists discovered a significant increase (decrease) of the Chinese Meiyu and Japanese Baiu rainfall during the summer after El Niño (La Niña) (Fu and Teng 1988; Zhang et al. 1996; Tao and Zhang 1998; Kawamura 1998). The key system that bridges this ENSO–East Asian Monsoon teleconnection is an anomalous Northwest Pacific surface anticyclone (cyclone) that forms in the late fall of the year El Niño (La Niña) develops and persists until the next summer (Harrison and Larkinn 1996; Wang et al. 2000). Although a variety of factors may initiate the anticyclone (cyclone) anomaly, a major reason for its development and maintenance is positive wind–sea surface temperature (SST) feedback (Wang et al. 2000; Wang and Zhang 2002). For El Niño scenario, the western Pacific cooling that accompanies the central Pacific warming induces the westward descending Rossby Wave. The strengthened northeasterly in the southern part of the anticyclone, superimposed on the tropical trade winds, reinforces the initial SST cooling via surface evaporation and wind stirring.

This so-called wind-evaporation–SST (WES)–V feedback (Xie et al. 2009), although robust throughout winter and spring, may go through a major transition in summer. Wang et al. (2005) showed that the positive precipitation–SST correlation that required by this mechanism becomes weak or even negative in June–August. This transition was further discussed by Wu et al. (2009), who introduced negative SST–solar radiation flux feedback which leads to the reverse of anomalous SST signs for the Northwest Pacific in El Niño decaying summer. On the other hand, the mean tropical surface winds that are crucial to the WES–V feedback change suddenly in spring and asymmetrically in the Northwest Pacific. As shown in Fig. 1a, b, an area with negative SST anomaly is found in the Northwest Pacific in spring (which is defined as NWPCA (125°E–170°E, 4°N–20°N) here) and is caused by the northeasterly winds which favor WES–V feedback.

H. Hu (✉) · J. He · Q. Wu
School of Atmospheric Sciences, Nanjing University, Nanjing 210093, China
e-mail: huhaibo@nju.edu.cn

Y. Zhang
School of Atmospheric Sciences, Nanjing University of Information Science and Technology, Nanjing, China

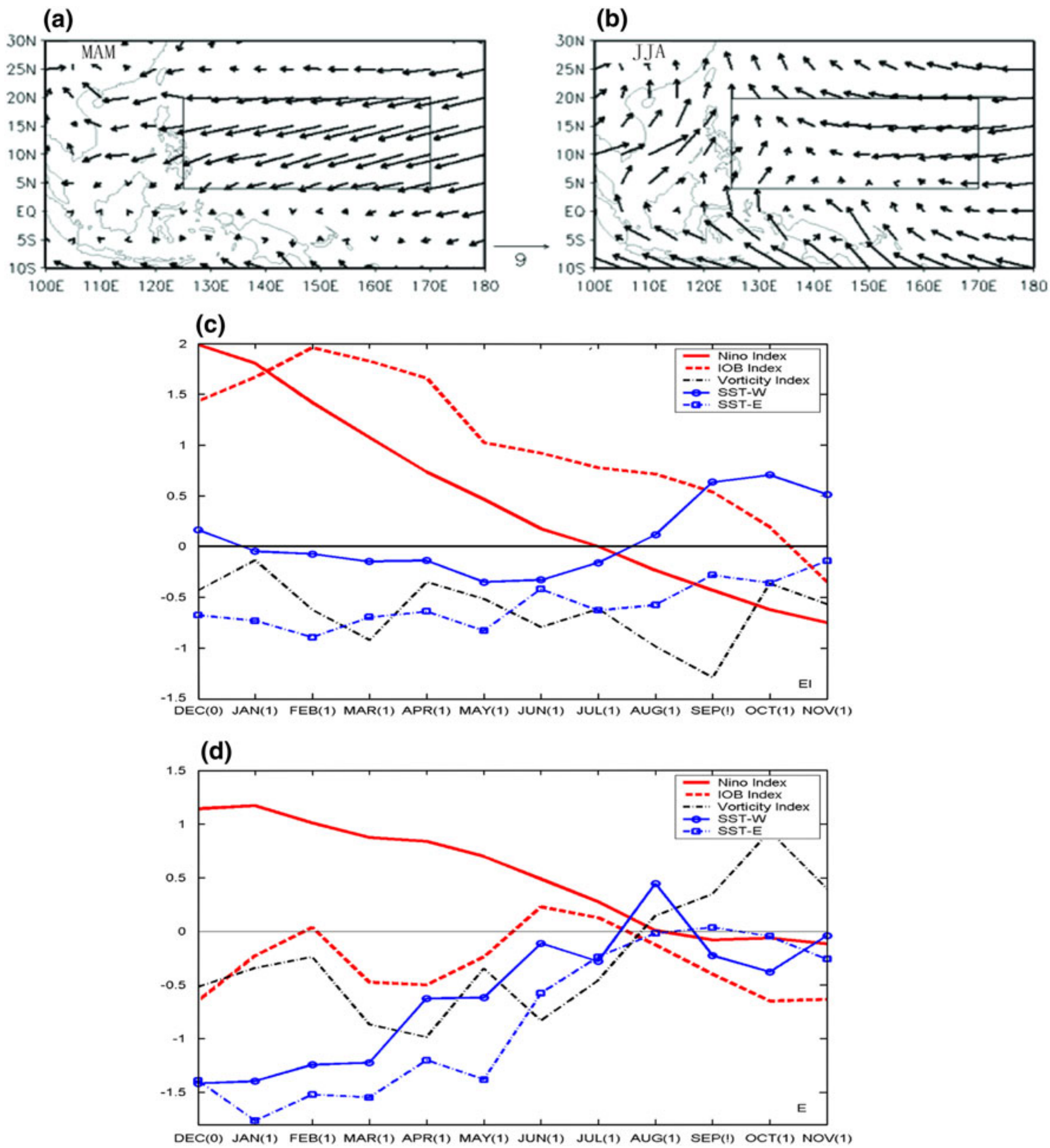

Fig. 1 Observed **a** March–April–May and **b** June–July–August mean surface winds. The *rectangles* indicate the anomalous Northwest Pacific cold area (125–170°E, 4–20°N). El Niño (*red unbroken line*), IOB warming (*red dashed line*), and vorticity (*black dot dashed line*) indices averaged over 125–170°E, 10–25°N and mean SST anomalies over the West NWPCA (SST–W indicated by the *blue unbroken line with filled circles*) and East NWPCA (SST–E indicated by the *blue real line with squares*) for **c** composite (EI) events and **d** composite (E) events (see text for (EI) and (E) events). All data have been normalized. *Numbers in parentheses* denote years relative to El Niño: *0* for its developing year and *1* for decaying year

In summer, the winds in the east NWPCA change only with the vanishing of the meridional component, whereas the northeasterlies in the west NWPCA either diminish or are replaced by adverse southwesterly monsoon winds. This zonal asymmetric transition of the background wind field indicates an asymmetric development of SST and wind anomalies, which will be discussed later in this paper.

Indian Ocean Basin (IOB) warming usually follows El Niño (Klein et al. 1999). It forces a warm eastward equatorial Kelvin wave to the south of the Northwest Pacific anticyclone, and strengthens the easterly wind via circulation–convection feedback (Xie et al. 2009). IOB warming also contributes to the maintenance of the anomalous Northwest Pacific anticyclone, especially in June–August when El Niño signal usually starts to disappear and IOB warming remains obvious (Yang et al. 2007). In observation and modeling studies, Xie et al. (2009) and Du et al. (2009) also show that IOB warming caused the easterlies, and then induced warming SST anomalies in the area west of the Northwest Pacific (including the South China Sea, SCS) in early summer. Although the Indian Ocean capacitor effect is compared with the local WES–V feedback in Xie et al. (2009), the detailed process of local ocean–atmosphere interaction in the Northwest Pacific has not been addressed, especially how IOB warming and the asymmetric background wind transition could affect the NWPCA.

The main purpose of our study was to investigate in detail the processes involved in the effect of IOB warming on the Northwest pacific SST anomalies, especially during the spring–summer climate transition season. We divide El Nino episodes into two groups, one followed by IOB warming and the other not followed by IOB warming. By comparing the Northwest Pacific SST anomaly and its coupling process with the Northwest Pacific anticyclone in the two groups, we isolated the possible remote effect of the Indian Ocean, with particular emphasis on its zonal asymmetric effect. The rest of this paper is organized as follows. The datasets and methods used are presented in the Sect. 2. Section 3 presents IOB's zonal asymmetric effect on Northwest Pacific based on observational analysis. Section 4 provides a summary of the results and discussion.

2 Data and methods

2.1 Data

The main datasets are from NCEP–NCAR re-analysis (Kalnay et al. 1996) and extended reconstruction sea surface temperature (ERSST.v3b) from 1950 to 2009 (Smith et al. 2008). Climate Prediction Center (CPC) merged analysis of precipitation (CMAP) data (Xie and Arkin 1996) from 1979 to 2009 are used. The climate for each month is removed separately for all fields. To reduce the effect of trends, linear trends were removed from the monthly anomalies by the least-squares fit at each grid point for all fields.

Our main strategy was to compare typical El Niño episodes that were followed by strong IOB warming with those that did not have significant subsequent IOB warming. Hereafter in this paper, these two categories will be referred to as (EI) and (E), respectively. Because no La Niña episode happened with clear absence of IOB cooling, we did not study the cold phase.

The principal-component time series associated with the leading EOF modes of SST variability over the tropical Pacific Ocean (120°E–60°W, 26°S–26°N) and the tropical Indian Ocean (30°E–120°E, 30°S–26°N) are defined as the Niño and IOB warming indices, respectively. We set the threshold of El Niño (IOB warming) episodes as the Niño (IOB) index exceeding its 0.75 standard deviation for 5 consecutive months. Accordingly, seven (EI) cases (1951/1952, 1957/1958, 1963/1964, 1972/1973, 1982/1983, 1987/1988, 1997/1998) and four (E) cases (1965/1966, 1991/1992, 1992/1993, 1994/1995) are identified for the period from 1950 to 2009. During the 2006/2007 El Niño episode, significant warm SST anomalies in the IOB were observed in the winter of 2006 and in the summer of 2007, but not in the spring of 2007. It is thus excluded in the (EI) cases. Virtually all El Niño and IOB warming episodes exhibit tight phase locking to the annual cycle, with El Niño maturing in December and fading toward the following May, and IOB warming evolving with an approximate 1 season's lag (not shown). To illustrate the zonal asymmetry of NWPCA in Fig. 1, we have defined the area where the easterly wind prevails in the spring–summer transition as the East NWPCA (145°E–170°E, 4°N–20°N), and the area where the East Asia Summer Monsoon circulation takes over as the West NWPCA (125°E–145°E, 4°N–20°N).

2.2 Latent heat flux decomposition

Latent heat flux variations involve changes in both atmospheric conditions and SST. Latent heat flux can be expressed as the sum of atmospheric forcing and oceanic response (De Szoeke et al. 2007; Du and Xie 2008; Du et al. 2009),

$$Q'_{\mathrm{E}} = Q'_{\mathrm{EA}} + Q'_{\mathrm{EO}}. \qquad (1)$$

The oceanic response arises from the dependence of SST on evaporation and may be cast as a Newtonian cooling term:

$$Q'_{\mathrm{EO}} = \overline{Q_{\mathrm{E}}}\beta T', \qquad (2)$$

where the overbar (prime) denotes the mean (perturbation), and $\beta = 1/q_s(dq_s/dT)$. The residual Q'_{EA} is regarded as atmospheric forcing in the whole latent heat flux (AtF-L), aroused by changes in wind speed, relative humidity, and air–sea temperature difference.

3 IOB's zonal asymmetric effect on the NW Pacific

3.1 The spring–summer transition

The evolution of the Northwest Pacific anticyclone and the NWPCA during El Niño decaying year has significant temporal distinctions in the composite (EI) and (E) events.

As shown in Fig. 1c, d, for both the (EI) and (E) composites, El Niño reaches its peak in winter and vanishes in the following summer. IOB warming only exists in the (EI) composite and persists until October (1). For both the (EI) and (E) events, the negative West NWPCA SST anomaly is caused by El Niño, and persists until El Niño signal disappears (between July (1) and August (1)), and the SST cooling for both events quickly turns positive for the following summer. The main differences between the (EI) and (E) composites are the amplitudes of vorticity anomalies (which indicate the strength of the Northwest Pacific anticyclone) and evolution of the East NWPCA SST anomaly during the transition season. In the composite (EI) events, the negative anomalous SST in the East NWPCA lasts almost throughout the entire decaying year of El Niño and shows no clear sign of weakening until IOB warming disappears after October (1). In the composite (E) events, however, the East NWPCA SST anomaly, consistently with the SST anomaly in the west part, rapidly diminishes to zero around August (1). Similarly, the decaying time for the Northwest Pacific anticyclone in (EI) shows a significant delay of 3 months compared with that in (E).

Therefore, the negative SST anomaly in the East NWPCA cannot survive during the decaying year summer without the presence of IOB warming. The Northwest Pacific anticyclone also has a much shorter lifespan in the (E) composite, and it starts to retreat just after the decay of El Niño index, whereas the Northwest Pacific anticyclone persists in the whole decaying summer in the (EI) composite. This indicates that IOB warming plays an important role in the summer coupling between SST and surface wind anomalies in the Northwest Pacific.

During the warm phase of the IOB, tropospheric air temperature increases over the entire tropical Indian Ocean through a moist-adiabatic adjustment (Emanuel et al. 1997). On the basis of observational and modeling results, Xie et al. (2009) concluded that this IOB warming forces an eastward tropical Kelvin wave which strengthens the easterly anomalies in the NW Pacific. This intensified easterly wind (Fig. 2) shows the different climate patterns in MAM (1) and JJA (1) for the (EI) and (E) composites. Compared with (E), the zonal component of the anomalous wind in the Northwest Pacific is stronger in the (EI) during both spring and summer. The cold SST anomaly in the

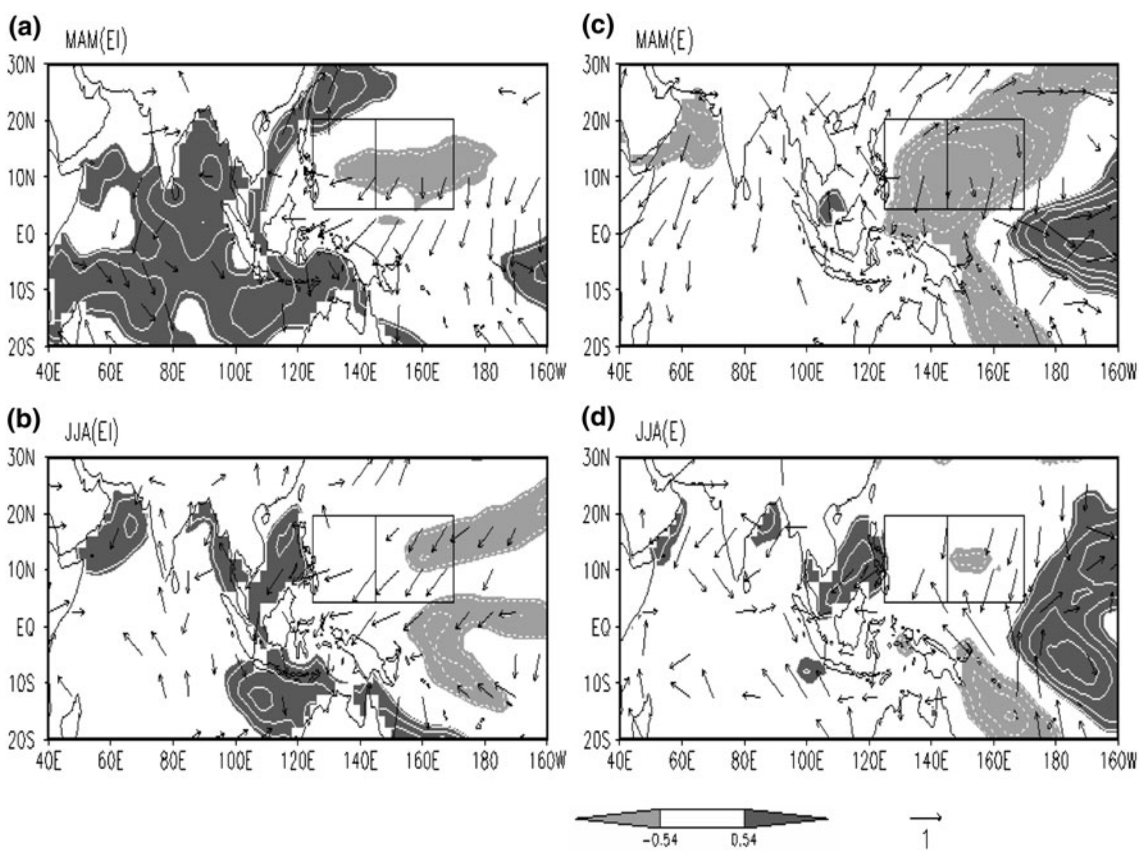

Fig. 2 MAM and JJA mean surface wind anomalies (*vectors*) and SST anomalies (*shaded*) for (EI) composites (**a** MAM, **b** JJA) and (E) composites (**c** MAM, **d** JJA). All data have been normalized. Winds that are <0.5 m s^{-1} in both zonal and meridional components are not shown. The contour interval for SST anomalies is 0.2°C. The *rectangles* indicate the West NWPCA (*left*) and the East NWPCA (*right*)

NWPCA shows a west-to-east retreat in the spring–summer transition. In summer, the cold signal disappears in the West NWPCA, whereas much of the cold signal is sustained in the east. In the (E) composite, by contrast, the cold SST anomalies nearly disappear in the whole NWPCA. Also noteworthy is an eastward shift of the Northwest Pacific anticyclone in Fig. 2a, b. Therefore, IOB warming facilitates continuation of the WES–V feedback after the seasonal climate transition, but only in the east part of NWPCA. So what is the zonal different process on the surface budget? And how is the anomalous anticyclone strengthened as a whole in the summer for the (EI) events (Fig. 1c)?

To understand these phenomena, we look back at the seasonal transition of mean surface winds shown in Fig. 1, which is also asymmetric in character. Because the easterly wind anomaly generated by IOB warming is only consistent with the tropical trade winds in the East NWPCA, and is inconsistent or even opposed to the monsoon circulation in the west, the total mean surface wind is intensified in the east and reduced in the west. This leads to asymmetry of the latent heat budget and, consequently, asymmetry of the SST pattern. When the zonal SST gradient is established, it may further increase the initial easterly wind anomalies and the strength of the Northwest Pacific anticyclone, especially in the East NWPCA.

3.2 The surface heat budget

Because of the deep mean thermocline in the WN Pacific warm pool, the capacity of the thermocline variation to change the local SST is relatively weak. The AtF-L and shortwave radiative flux are the most dominant factors for the local SST evolution. To examine the different surface heat budgets associated with the anomalous wind patterns during the (EI) and (E) events, we present in Fig. 3 the summer AtF-L anomalies, zonal wind anomalies, and SST anomalies in the east and west NWPCA, and the solar radiation anomalies and vorticity anomalies in the NW Pacific.

For the West NWPCA, the (EI) and (E) composites show no fundamental difference in all variables. Although the easterly anomaly is greater in the presence of IOB warming than the (E) composite, both easterly anomalies reduce the background southwesterly monsoon wind, and consequently the local AtF-L loss. In addition, for both the (EI) and (E) events, the downward solar radiation is increased because of the decrease in the amount of cloud caused by local cold SST and anticyclonic wind suppressed convection (Wu et al. 2009). So both these two kinds of heat flux lead to a total positive energy budget anomaly and the retreat of the cold SST anomaly in the West NWPCA. Thus, local negative feedback exists between the cold SST anomaly and the anticyclone surface easterly wind anomaly.

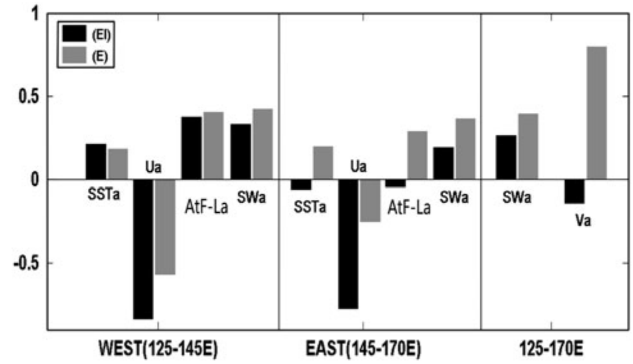

Fig. 3 The (EI) and (E) composite anomalies of SST (SSTa, °C), zonal wind (Ua), atmospheric forcing component of LHF (AtF-La), shortwave radiative flux (SWa) for WEST (125°E–140°E) and EAST (140°E–170°E), and the SWa and vorticity anomaly (Va) in the whole NWPCA (125°E–170°E) during JJA at 4°N–20°N. The SSTa and Va are calculated using a one order central difference scheme for each month (from June to August). To unify different variables to the order of 10^0, we multiply AtF-La and SWa by 0.1 W m^{-2} and Va by 5 × 10^5 s^{-1} $month^{-1}$

In the East NWPCA, by contrast, the (EI) and (E) composites differ dramatically. The anomalous easterly is significantly weaker in the (E) composites. Because the cold SST anomalies restrain convection, the anomalous solar radiation and AtF-L are still positive and the ocean surface gets warmer. In the (EI) composites, however, the anomalous easterly is remotely intensified by IOB warming, and brings a plentiful AtF-L loss from the East NWPCA. Although there is still a very weak positive solar radiation anomaly (the weak positive solar radiation mainly appears in the West NWPCA), the total heat budget is able to remain negative and the cold SST anomaly is sustained. Thus, local positive feedback exists between the cold SST anomaly and the anticyclone surface easterly wind anomaly in the East NWPCA.

4 Summary and discussion

In this study, we have investigated the evolution of Northwest Pacific SST–wind feedback with/without the effect of IOB warming in the spring–summer transition. While the IOB warming-induced easterly anomaly prevails over the NWPCA, it sets off zonal asymmetry ocean–atmosphere feedbacks in the context of the zonal asymmetric background wind, which eventually contribute to the anomalous anticyclone in the Northwest Pacific. We summarize this mechanism with a schematic diagram shown in Fig. 4.

In both the West and East NWPCA, cold SST anomalies start in the spring–summer transition time and induce the

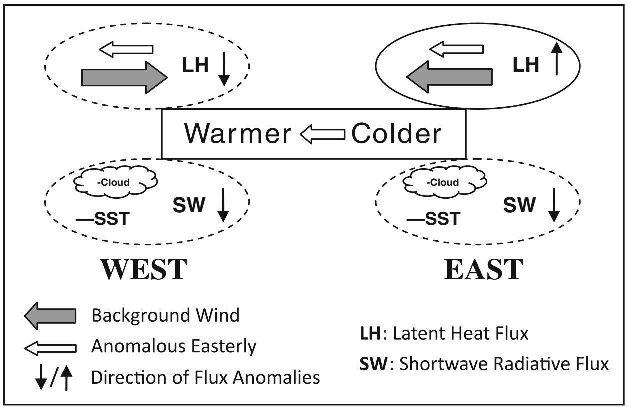

Fig. 4 Schematic diagram showing the asymmetric process that intensifies the easterly anomalies in the NWPCA during the (EI) summer. *Ellipses with dashed outlines* indicate processes that cause the SST to increase, and the *ellipse with a solid outline* indicates the opposite. In the *rectangle* is the positive feedback that intensifies the anomalous easterlies

negative SST–cloud–solar radiation feedback that warms the sea surfaces. Meanwhile, IOB warming forces anomalous easterlies over the NWPCA, and these act to weaken the southwest monsoon wind in the west but strengthen the east tropical trade wind in the east. As a result, a negative WES–V feedback takes over in the West NWPCA, accelerating local sea surface warming, while the positive WES–V feedback continues to cool the East NWPCA. This zonal asymmetric transition of air–sea interaction leads to an east–west SST gradient, which also intensifies the initial anomalous easterly and eventually maintains the anticyclone anomaly.

We have noticed two interesting phenomena that should be relevant to this study. First, the warm pool in the SCS extends eastward during the spring–summer transition time (Fig. 2). Similar to the West NWPCA, this SCS is dominated by southwest monsoon wind during June–August (Fig. 1b). Reasonably, the same negative WES–V feedback works there to warm the local sea surface, as discussed by Xie et al. (2009) and Du et al. (2009). Therefore, if the SCS is included, the zonal asymmetric effect of IOB warming would be even more manifest, and its contribution to intensifying the easterly anomaly is more significant than we have proposed.

Second, the cold SST anomaly in the Northwest Pacific is much stronger during winter and spring without the presence of IOB warming than that in the (EI) composite (Fig. 1d). This seems contradictory to the positive effect of IOB warming on the Pacific. According to Annamalai et al. (2005), however, IOB warming is able to weaken the ongoing El Niño by generating the equatorial easterly that strengthens the tropical Pacific Walker Circulation (partly shown in Fig. 2a, c). Thus, IOB warming actually suppresses the development of the NWPCA before the spring–summer transition time. Its positive effect only starts during the transition season when El Niño is no longer the leading factor and the zonal asymmetric mechanism discussed above begins to take its place.

Acknowledgments This work is supported by the National Natural Science Foundation of China (40906005; GYHY201106017); the National Key Program for Developing Basic Science (2010CB428504); and the National Key Technologies R&D Program of China under Grant 2009BAC51B01.

References

Annamalai H et al (2005) Impact of Indian Ocean sea surface temperature on developing El Niño. J Clim 18:302–319

De Szoeke D et al (2007) What maintains the SST front north of the eastern Pacific equatorial cold tongue. J Clim 20:2500–2514

Du Y, Xie S-P (2008) Role of atmospheric adjustments in the tropical Indian Ocean warming during the 20th century in climate models. Geophys Res Lett 35:L08712. doi:10.1029/2008GL033631

Du Y et al (2009) Role of air–sea interaction in the long persistence of El Nino-induced North Indian Ocean warming. J Clim 15:2023–2038

Emanuel K et al (1997) Reply to comments by Bjorn Stevens, David A. Randall, Xin Lin and Michael T. Montgomery on 'On large-scale circulations in convecting atmospheres'. Quart J R Meteorol Soc 123:1779–1782

Fu C, Teng X (1988) The relationship between ENSO and climate anomaly in China during the summer time. Sci Atmos Sin 12:133–141

Harrison D, Larkinn NK (1996) The COADS sea level pressure signal: a near-global El Niño composite and time series view 1946–93. J Clim 9:3025–3055

Kalnay E et al (1996) The NCEP/NCAR 40-year reanalysis project. Bull Am Meteorol Soc 77:437–471

Kawamura R (1998) A possible mechanism of the Asian summer monsoon–ENSO coupling. J Meteorol Soc Jpn 76:1009–1027

Klein SA et al (1999) Remote sea surface temperature variations during ENSO: evidence for a tropical atmospheric bridge. J Clim 12:917–932

Smith TM et al (2008) Improvements to NOAA's historical merged land-ocean surface temperature analysis (1880–2006). J Clim 21:2283–2296

Tao S, Zhang Q (1998) Response of the East Asian summer monsoon to ENSO events. Sci Atmos Sin 22:399–407 (in Chinese)

Wang B, Zhang Q (2002) Pacific-East Asia teleconnection. Part II: How the Philippine Sea anomalous anticyclone is established during El Niño development. J Clim 15:3252–3265

Wang B et al (2000) Pacific-East Asia teleconnection: how does ENSO affect East Asian climate? J Clim 13:1517–1536

Wang B et al (2005) Fundamental challenge in simulation and prediction of summer monsoon rainfall. Geophys Res Lett 32:L15711. doi:10.1029/2005GL022734

Wu B et al (2009) Contrast of rainfall-SST relationships in the Western North Pacific between the ENSO-developing and ENSO-decaying summers. J Clim 22:4398–4405

Xie P, Arkin PA (1996) Analyses of global monthly precipitation using gauge observations, satellite estimates, and numerical model predictions. J Clim 9:840–858

Xie S-P et al (2009) Indian Ocean capacitor effect on Indo-Western Pacific climate during the summer following El Niño. J Clim 22:730–747

Yang J et al (2007) Impact of the Indian Ocean SST basin mode on the Asian summer monsoon. Geophys Res Lett 34:L02708. doi:10.1029/2006GL028571

Zhang R et al (1996) Impact of El Niño on the East Asian monsoon: a diagnostic study of the ’86/87 and ’91/92 events. J Meteorol Soc Jpn 74:49–62